THE JOURNAL OF PROSTHETIC DENTISTRY

RESEARCH AND EDUCATION

Dual-phase deep learning recommendation system for radiographic crown lengthening assessment and post selection for the restoration of endodontically treated teeth

Mohamed Mostafa Rezk, BSc,[a] Lamiaa Said ElFadaly, BDS, MSc, PhD,[b] and Zeinab Abd Elhalim Taha, BSc, MSc, PhD[c]

ABSTRACT

Statement of problem. Restoring endodontically treated teeth requires careful evaluation of the supracrestal tissue attachment, ferrule integrity, and post-space dimensions to ensure long-term success. Manual radiographic analysis for crown lengthening indication and post selection is often time-consuming, subjective, and inconsistent, particularly in resource-limited settings where specialist access may be constrained.

Purpose. The purpose of this study was to design and validate an artificial intelligence (AI)–driven system that automated 2 essential restorative planning tasks, evaluating the clinical need for crown lengthening and recommending appropriate post dimensions in endodontically treated teeth, using dental radiographs as the input.

Material and methods. Two deep learning pipelines were developed and trained on annotated panoramic and periapical datasets with annotations created under the supervision of dentistry professionals. The crown measurement pipeline employed a U-shaped network (U-Net) model for initial tooth segmentation (assigning unique instance masks to each tooth), then cropping individual teeth and feeding them into a Mask Region-based Convolutional Neural Network (Mask R-CNN) for precise detection and crown length calculation, facilitating the assessment of parameters such as supracrestal tissue attachment and ferrule height, for identification of potential violations or restoration limitations. The post measurement pipeline utilized Mask R-CNN directly on the original images to detect endodontic posts and measure their length and width, enabling comparison against established prosthodontic criteria. Both models were trained in a graphics processing unit (GPU)-enabled environment (Kaggle; Google LLC) and evaluated using standard metrics including Intersection over Union (IoU), Dice coefficient, and measurement accuracy, with validation involving visual overlays and quantitative comparisons to expert annotations.

Results. The segmentation model achieved a mean IoU of 0.52 and a Dice coefficient of 0.66, with diagnostic accuracy exceeding 99% in identifying post locations and assessing ferrule presence. The system accurately detected supracrestal tissue attachment violations and provided clinically relevant post dimension recommendations, closely aligning with expert-guided decisions. GPU acceleration reduced model training time by over 70% compared to local central processing unit (CPU)-only workflows.

Conclusions. The AI-powered system demonstrated promising performance in automating radiographic evaluations critical to restoring endodontically treated teeth. By identifying crown lengthening requirements and suggesting post dimensions, the integrated pipelines supported objective and reproducible treatment planning. This approach may enhance prosthodontic workflows, especially in settings with limited specialist availability, and holds potential for integration into commercial dental imaging platforms. (J Prosthet Dent xxxx;xxx:xxx-xxx)

The restoration of endodontically treated teeth with subgingival caries or fractures presents a dual challenge: achieving sufficient sound tooth structure for predictable retention and resistance form while maintaining periodontal health, particularly when margins must be placed subgingivally.[1] Crown lengthening is a

The authors declare that they have no known competing financial interests or personal relationships that could have appeared to influence the work reported in this paper.
[a]Graduate student, Faculty of Computer Science, October University for Modern Sciences & Arts, Cairo, Egypt.
[b]Assistant Professor, Faculty of Dentistry, Department of Prosthodontics, October University for Modern Sciences & Arts, Cairo, Egypt.
[c]Assistant Professor, Faculty of Computer Science, October University for Modern Sciences & Arts, Cairo, Egypt.

Clinical Implications

An artificial intelligence–based decision support system that automates crown lengthening assessment and post selection in endodontically treated teeth may enhance diagnostic consistency, reduce chair time, and optimize restorative outcomes. This system has the potential to standardize treatment planning in prosthodontics, particularly in settings with limited specialist availability.

periodontal surgical procedure performed to increase supragingival tooth structure for restorative and/or esthetic purposes, typically through apically positioned flap procedures and, when indicated, osseous resection or recontouring.[2] Functional crown lengthening has been undertaken to prevent restorative margin encroachment on the supracrestal tissue attachment and to facilitate creation of an adequate ferrule by exposing sound tooth structure for margin placement, thereby improving restorative prognosis.[3]

The supracrestal tissue attachment comprises the junctional epithelium and supracrestal connective tissue attachment coronal to the alveolar crest; classic histology reports mean dimensions of approximately 0.97 mm and 1.07 mm, respectively (total about 2.04 mm), with biologic variability.[4] Margin violation has been associated with persistent inflammation and periodontal breakdown (attachment and bone loss), particularly when plaque control is compromised around subgingival margins.[1] Accordingly, approximately 3 mm from the restorative margin to the alveolar crest has been commonly recommended to accommodate the supracrestal attachment and sulcus; when inadequate, crown-lengthening surgery may be required before definitive margin placement.[5]

The ferrule effect, a circumferential band of sound tooth structure ideally 1.5 to 2.0 mm, improves the fracture resistance of endodontically treated teeth under occlusal loads.[6–11] Achieving a 1.5 mm ferrule often requires approximately 4.5 mm of supragingival tooth structure when supracrestal attachment and sulcus dimensions are considered.[12] If coronal structure is insufficient, options include surgical crown lengthening, orthodontic extrusion, or surgical extrusion.[13–15] However, decisions regarding the need for crown lengthening and the extent of osseous reduction are patient-specific and rely on clinical measurements and radiographic evaluation[16]; both are limited by examiner variability[17,18] and projection-related distortion from tube angulation and sensor alignment in 2-dimensional (2D) imaging.[19]

Advances in digitally assisted dentistry have improved procedural precision. Digitally designed surgical guides can direct gingivectomy and ostectomy for crown lengthening with high accuracy, and guided surgery is more accurate than freehand approaches.[20] However, guide design still depends on accurate evaluation of supracrestal tissue attachment and ferrule feasibility, where artificial intelligence (AI) could enhance standardization.

Intraradicular post selection has been reported to strongly influence long-term outcomes in endodontically treated teeth. Standard guidance emphasizes maximizing retention while preserving radicular dentin and the apical seal, typically recommending a post length of approximately two-thirds of the canal (or at least the clinical crown length) while maintaining 4 to 5 mm of apical gutta percha.[21–23] Post diameter is kept conservative (often no greater than one-third of the root diameter), and prognosis has been reported to improve when a circumferential ferrule of approximately 1.5 to 2.0 mm of sound tooth structure is present above the finish line.[24] However, estimating post length, diameter, remaining dentin thickness, and ferrule feasibility from periapical radiographs is difficult because 2D imaging is prone to overlap and angulation-related distortion.[25] Clinician surveys indicate that many post decisions still depend on radiographic estimation and rule-based heuristics,[26] highlighting an opportunity for AI to extract patient-specific radiographic measurements (root and canal length, crown height, dentin thickness, projected ferrule) and deliver more consistent, evidence-aligned recommendations in line with broader AI-assisted radiographic interpretation.[27]

AI has rapidly expanded in dentistry over the past decade, demonstrating capabilities in radiographic diagnosis, treatment planning, and even execution of technical tasks.[20] In prosthodontics and restorative dentistry, recent AI applications include detection of crown preparation finish lines,[28] evaluation of crown designs and marginal fit.[29] Deep learning models, particularly convolutional neural networks (CNNs), can learn to recognize complex patterns in dental images that correlate with anatomical landmarks or pathologies. For example, CNNs have been used to segment structures on intraoral radiographs with high accuracy, including detecting apices, alveolar bone levels, and periodontal bone loss patterns.[30–32] In endodontics, AI models can identify root canal outlines and predict working lengths to within an error of 0.2 to 0.3 mm,[33] rivaling the precision of electronic apex locators. Currently, periapical radiograph assessment for crown lengthening or post selection relies on the clinician's measurement and judgment. Mistakes in estimating distances (such as bone level to crown margin or remaining root length) can lead to under- or over-treatment. AI algorithms offer a means to obtain precise, reproducible measurements and standardized recommendations in these situations. These advances

suggest that a well-trained deep learning model could similarly measure tooth and bone dimensions on a radiograph to inform crown lengthening and post selection decisions.

The present study proposed and evaluated a dual AI-based system to aid restorative treatment planning for endodontically treated teeth. The first component was a deep learning model that analyzed radiographs to determine if crown lengthening was needed for a given tooth and how much bone removal was required, based on the supracrestal tissue attachment and ferrule criteria. The second component was an AI algorithm that measured root and crown lengths from radiographs of endodontically treated teeth and recommended an optimal post size (length and, potentially, diameter) in accordance with the patient's anatomy. The research hypothesis was that these AI models can perform these tasks with accuracy comparable to experienced clinicians, thus providing a reliable decision support tool. Performance metrics including segmentation accuracy (Dice score and IoU for radiographic landmark identification), classification accuracy in decision-making, and measurement errors in millimeters (mm) were also reported. The feasibility of integrating AI into routine prosthodontic workflow for improved consistency and outcomes was explored to determine how automated image analysis can enhance clinical decision-making in crown lengthening and post-and-cores.

MATERIAL AND METHODS

A total of 2158 periapical radiographs[34,35] and 598 panoramic radiographs[36,37] were collected in collaboration with the Faculty of Dentistry and validated by experienced dentists for clinical correctness and image quality. For post measurement, the Mask Region-based Convolutional Neural Network (Mask R-CNN) model was applied to full periapical images, and the dataset was split into 70% training (1510), 20% validation (432), and 10% testing (216). For crown measurement, a U-shaped network (U-Net) segmentation model was applied to panoramic radiographs to enable tooth cropping (12 180 tooth instances), from which 1000 representative instances were selected to train and evaluate the downstream Mask R-CNN model. All radiographs were manually annotated to generate ground-truth labels for each task, including tooth outlines for segmentation and bounding boxes with class labels for crown-lengthening related structures and post location. All labels were reviewed for internal consistency before model training. Ethics approval had been obtained from the Research Ethics Committee of the Faculty of Dentistry, October University for Modern Sciences and Arts (REC-D 1123-6) for use of patient-derived radiographs.

A standardized preprocessing pipeline was applied across both tasks, including resizing images to a uniform resolution, normalization, and augmentation (rotation,

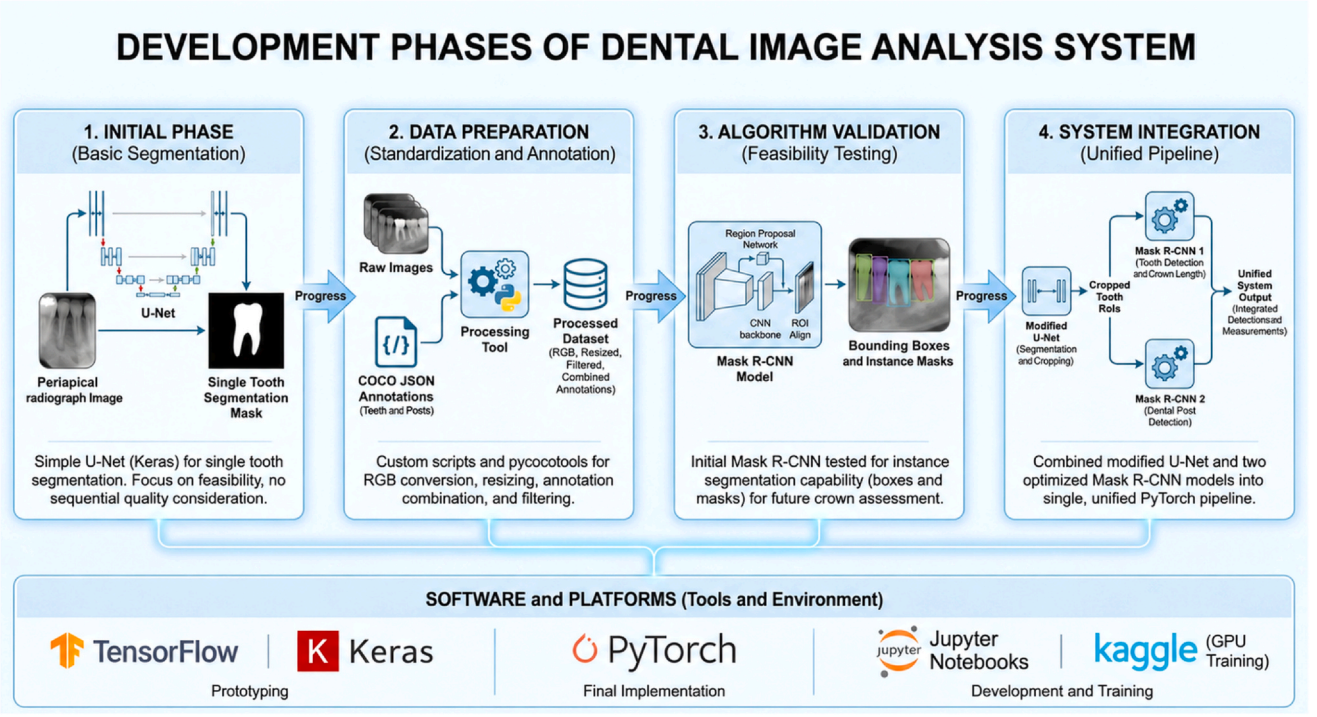


Figure 1. System development phases.

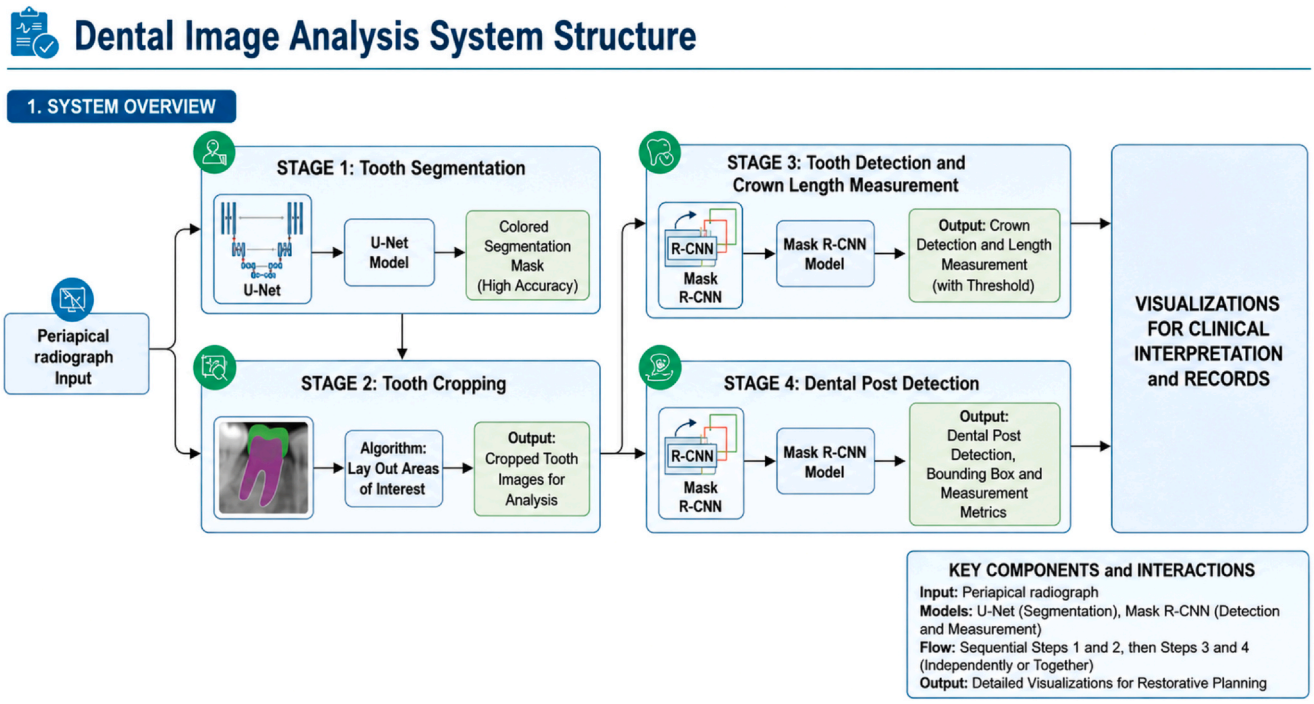


Figure 2. System architecture.

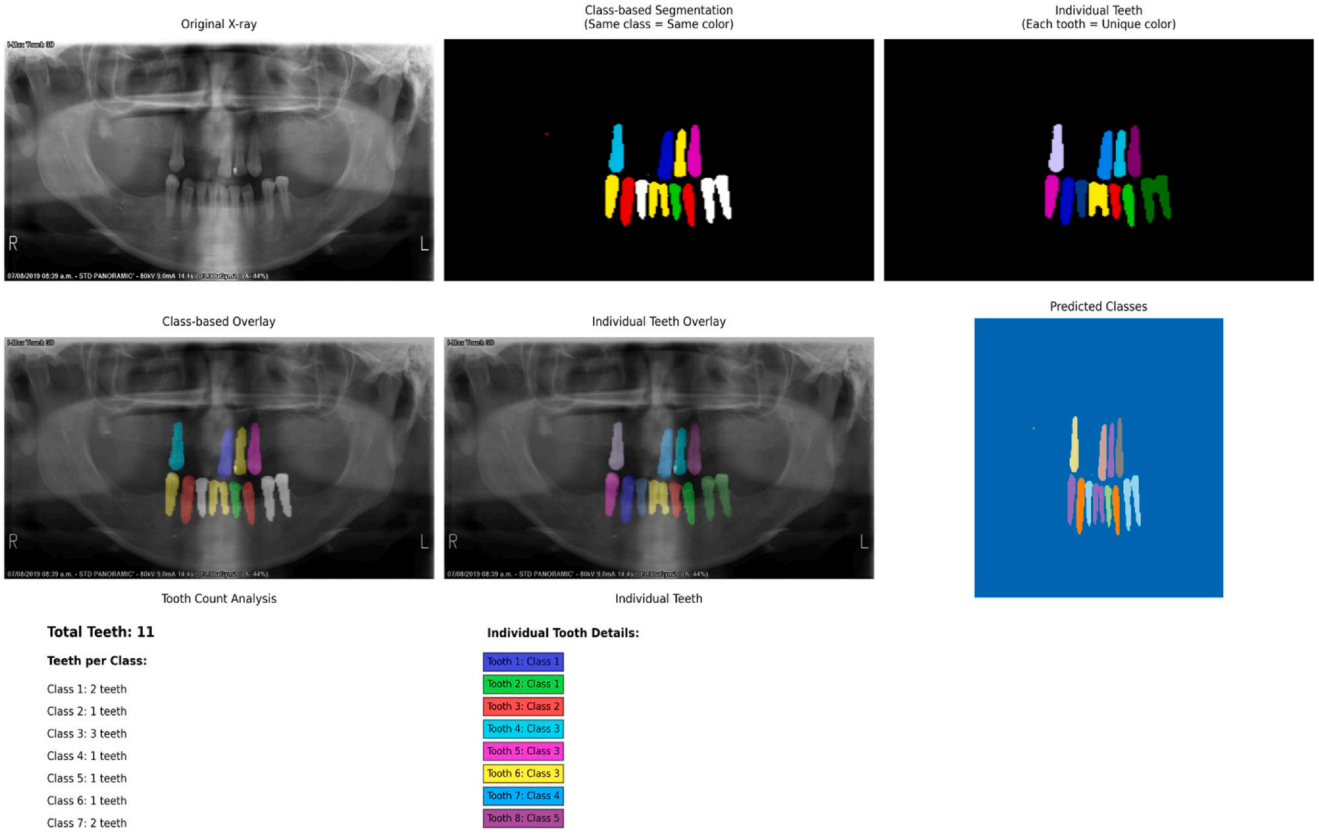


Figure 3. U-Net test results. U-Net, U-shaped network.



Figure 4. Examples of tooth cropping.

flipping, and contrast adjustment). The same transformations were applied to corresponding masks to preserve spatial alignment. A data-preparation module standardized images to red, green, and blue (RGB) format when required, integrated Common Objects in Context (COCO) formatted annotations using an application programming Interface (pycocotools; COCO Consortium), removed inconsistent annotations, and curated training-efficient subsets.

The computational workflow was developed in distribution (Anaconda Distribution; Anaconda Inc) using a programming language (Python 3; Python Software Foundation). Deep-learning model development used a framework (TensorFlow; Google LLC) and a high-level neural network application programming interface (Keras; Keras.io) during prototyping and a framework (PyTorch; Meta Platforms Inc) in the final implementation. Additional tools included a machine learning library (scikit-learn; scikit-learn.org), a computer vision library (OpenCV; OpenCV.org), an augmentation library (Albumentations; Albumentations.ai), a plotting library (Matplotlib; Matplotlib.org), and an imaging library (Pillow; Python Imaging Library), with supplementary utilities from the Python standard library (shutil, os, and glob) and a progress-bar utility (tqdm; tqdm.dev). Development was conducted in a notebook environment (Jupyter Notebook; Project Jupyter). Initial testing was performed on a processor (Intel Core i7-11370H; Intel Corp), and large-scale training was performed on a cloud platform (Kaggle; Google LLC) using graphics processing units (NVIDIA T4; NVIDIA Corp) with graphics processing unit (GPU) acceleration.[38,39] System development followed a staged approach. A preliminary U-Net model was implemented to generate single-tooth segmentation masks used for subsequent cropping. Mask R-CNN was then evaluated for its ability to produce reliable bounding boxes and masks to support crown-length assessment. The final integrated system combined a modified U-Net for segmentation and cropping with 2 task-specific Mask R-CNN models: 1 for tooth detection and crown-length measurement and 1 for dental post detection, forming a unified automated pipeline (Figs. 1, 2).

In the U-Net segmentation component, the input was a grayscale periapical radiograph in Portable Network Graphic (PNG) or Joint Photographic Experts Group (JPEG) format, typically resized to 512×512 pixels, and the output was a colored segmentation mask of the same dimensions in which each tooth was assigned a distinct RGB label (Fig. 3). The cropping component used the segmentation mask and the original radiograph to extract individual teeth, producing isolated grayscale PNG images that varied by tooth size but typically measured approximately 100×200 pixels (Fig. 4). For tooth detection and crown-length

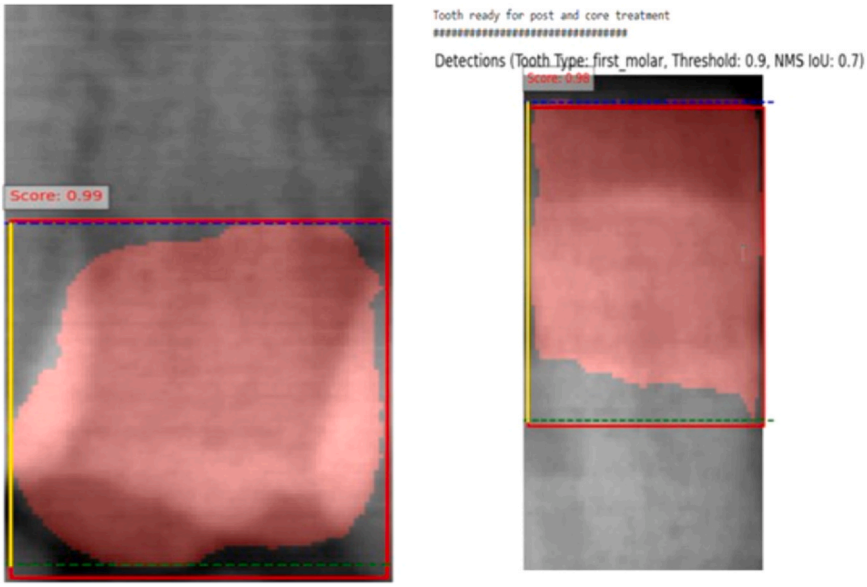
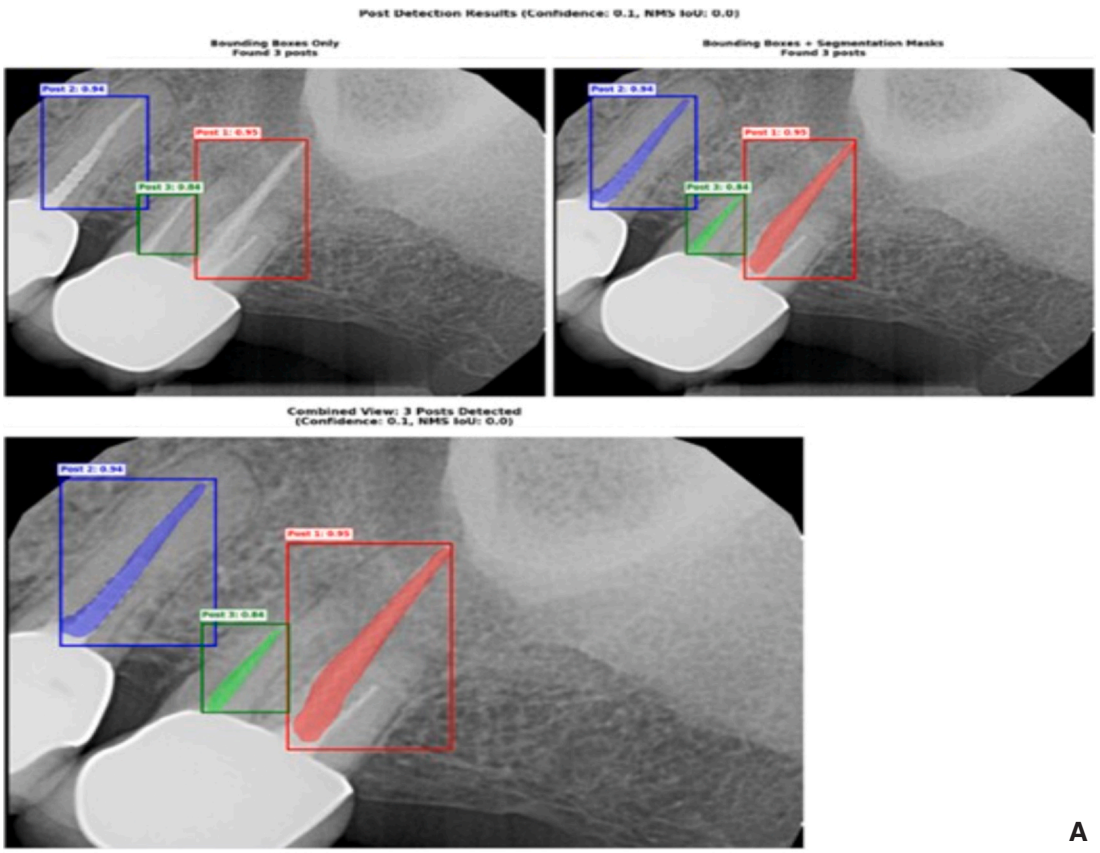


Figure 5. Crown lengthening detection results.



Prediction Results - Found 1 posts:

Post 1:
Box: [192.50677 75.84441 276.12912 502.05334]
Label: 1
Score: 0.920
Mask shape: (1, 844, 660)
height(mm): 8.90 mm
height(px): 424 pixels
width at adjusted top(mm): 0.36 mm
width at adjusted top(px): 17 pixels
adjusted top(px): 316
width at adjusted bottom(mm): 0.40 mm
width at adjusted bottom(px): 19 pixels
adjusted bottom(px): 264
color: red
Recommended fiber post: Size 0 (white)



Figure 6. Dental post detection. A, Segmentation of post space. B, Detection of post size.

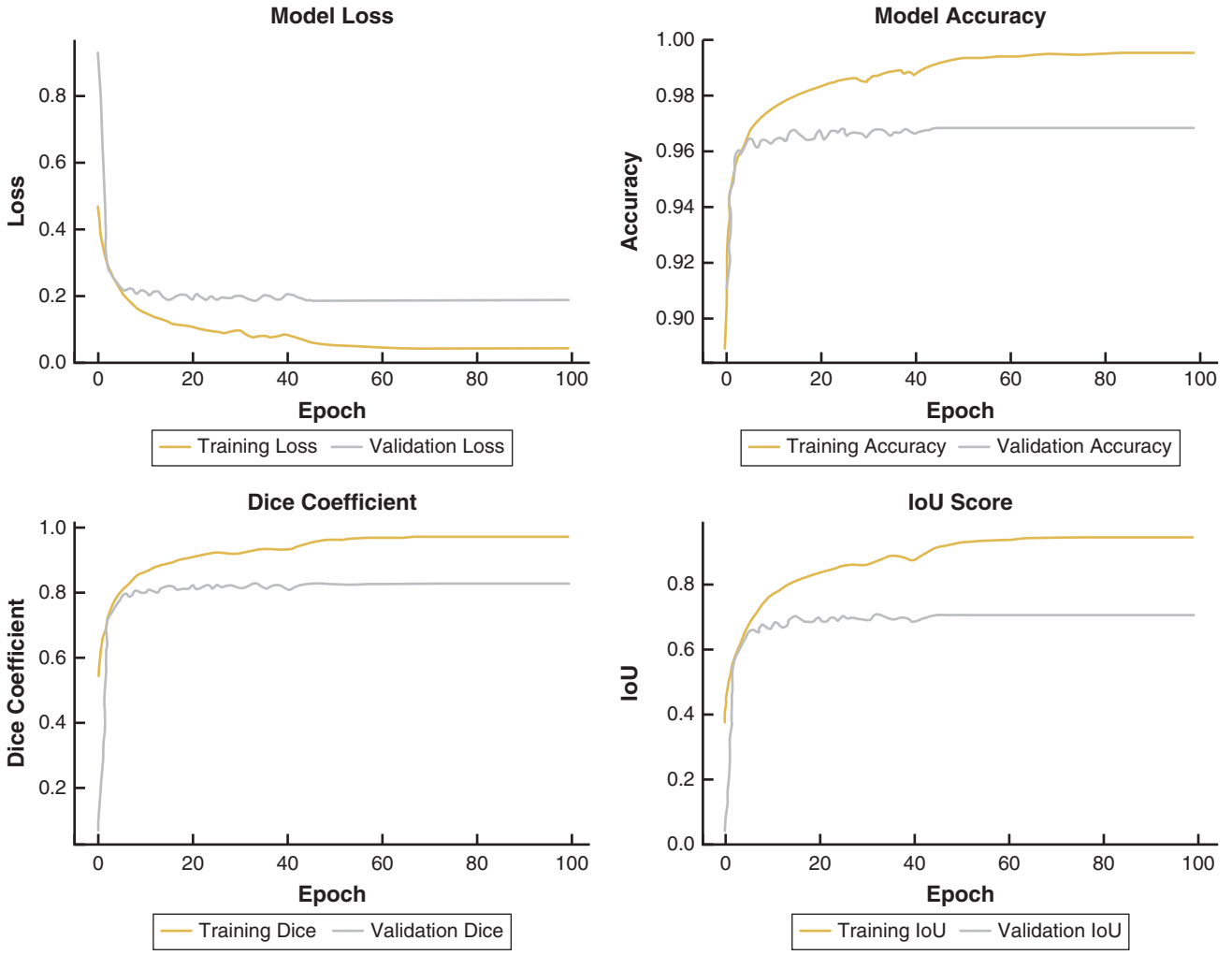


Figure 7. U-net training matrix result. U-Net, U-shaped network.

measurement, the Mask R-CNN model received either the original grayscale periapical radiograph or an individual cropped tooth image (PNG or JPEG), converted the input to an RGB tensor, and typically resized it to 512×512 pixels. The output included bounding box coordinates (x_1, y_1, x_2, y_2), binary masks, confidence scores, and crown-length values, together with text-based recommendations such as "Crown lengthening needed" or "Ready for post and core" (Fig. 5). For dental post detection, the Mask R-CNN model received a grayscale periapical radiograph (PNG or JPEG), converted it to an RGB tensor, typically resized it to 512×512 pixels, and output bounding box coordinates ([x_1, y_1, x_2, y_2]), binary masks, confidence scores, and bounding-box dimensions (width, height, and area in pixels; for example, 50×150 pixels with an area of 7500) (Fig. 6). The system additionally computed geometric descriptors from the predicted mask and box, including post height and coronal and apical width (reported in pixels and converted to millimeters) to support post-size selection.

Two Mask R-CNN segmentation pipelines were used for quantitative planning from periapical radiographs. First, fiber posts were segmented and refined (edge rejection, nonmaximum suppression, area-overlap suppression). Measurements were converted using a calibrated scale (0.021 mm/pixel), with post length derived from the vertical span of the post mask and coronal and apical diameters derived from maximal horizontal chords measured approximately 5 mm from each end (inverse scale factor) to reduce taper-related artifacts, enabling standardized post-size recommendations. Second, anatomical crown length was estimated using marker-free calibration. The user selected tooth type and population reference widths (for example, first molar 10.75 mm; central incisor 5.75 mm)[40] to compute an image-specific pixels-per-millimeter factor from mesiodistal bounding box width; then the tooth-mask vertical span was converted to crown length. Values less than 4.5 mm indicated additional tooth preparation.

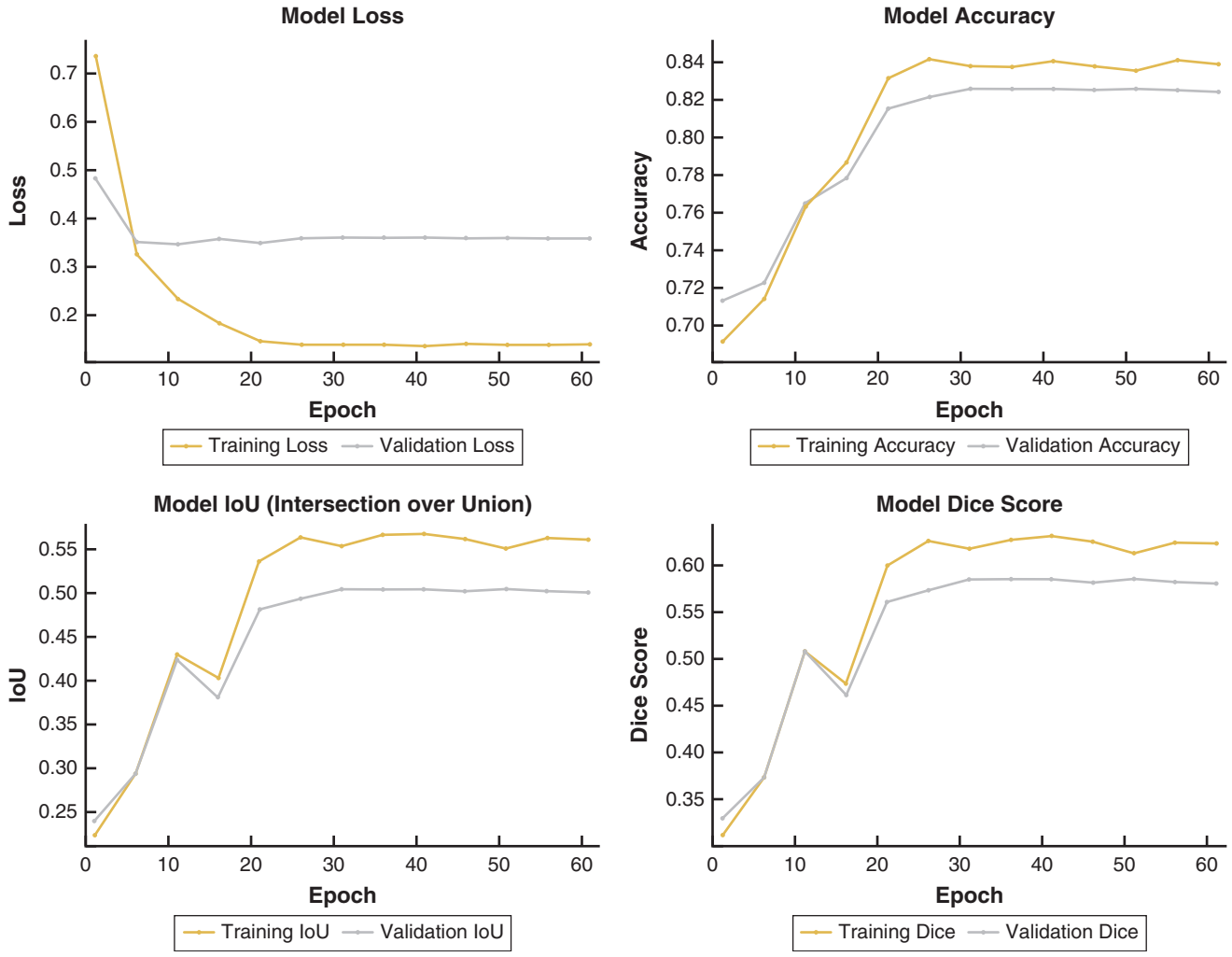


Figure 8. Mask R-CNN dental crown training matrix results. Mask R-CNN, region-based convolutional neural network.

RESULTS

Testing was conducted on all components of the system U-Net tooth segmentation, tooth cropping, tooth detection with crown-length measurement (Mask R-CNN), and dental post detection (Mask R-CNN), both individually and as a unified pipeline to ensure reliable performance in periapical radiograph analysis for restorative dentistry. The COCO-annotated dental radiograph dataset was divided into 70% for training, 20% for validation, and 10% for testing, with separate lesion annotations for teeth and posts to support component-level evaluation. The U-Net model was trained with a hybrid binary cross-entropy and Dice loss function and was evaluated using the Dice coefficient and pixel-wise accuracy (Fig. 7). The 2 Mask R-CNN models were trained with a composite loss function incorporating classification, bounding-box regression, mask generation, and region proposal network terms and were evaluated with intersection over union (IoU), Dice coefficient, and accuracy metrics. By epoch 79, post-detection performance reached an IoU of 0.5237, a Dice coefficient of 0.6588, and an accuracy of 0.9942 (Figures 8, 9, Table 1). Batch sizes of 8 for U-Net and 4 for the Mask R-CNN models were selected to accommodate graphics processing unit (GPU) memory constraints while maintaining stable gradients within the Kaggle environment with Compute Unified Device Architecture (CUDA), a parallel computing platform (CUDA; NVIDIA Corp), enabling acceleration. Validation was performed at the end of each epoch to monitor training convergence, whereas the test set was reserved for final evaluation of segmentation masks, cropped-tooth images, detection bounding boxes, crown-length measurements, and post-dimension outputs. Qualitative visualizations and quantitative assessment confirmed correct automation and supported the clinical relevance of the system's outputs (Figures 10, 11, Table 2).

Time performance was evaluated by comparing GPU training on Kaggle with local central processing unit

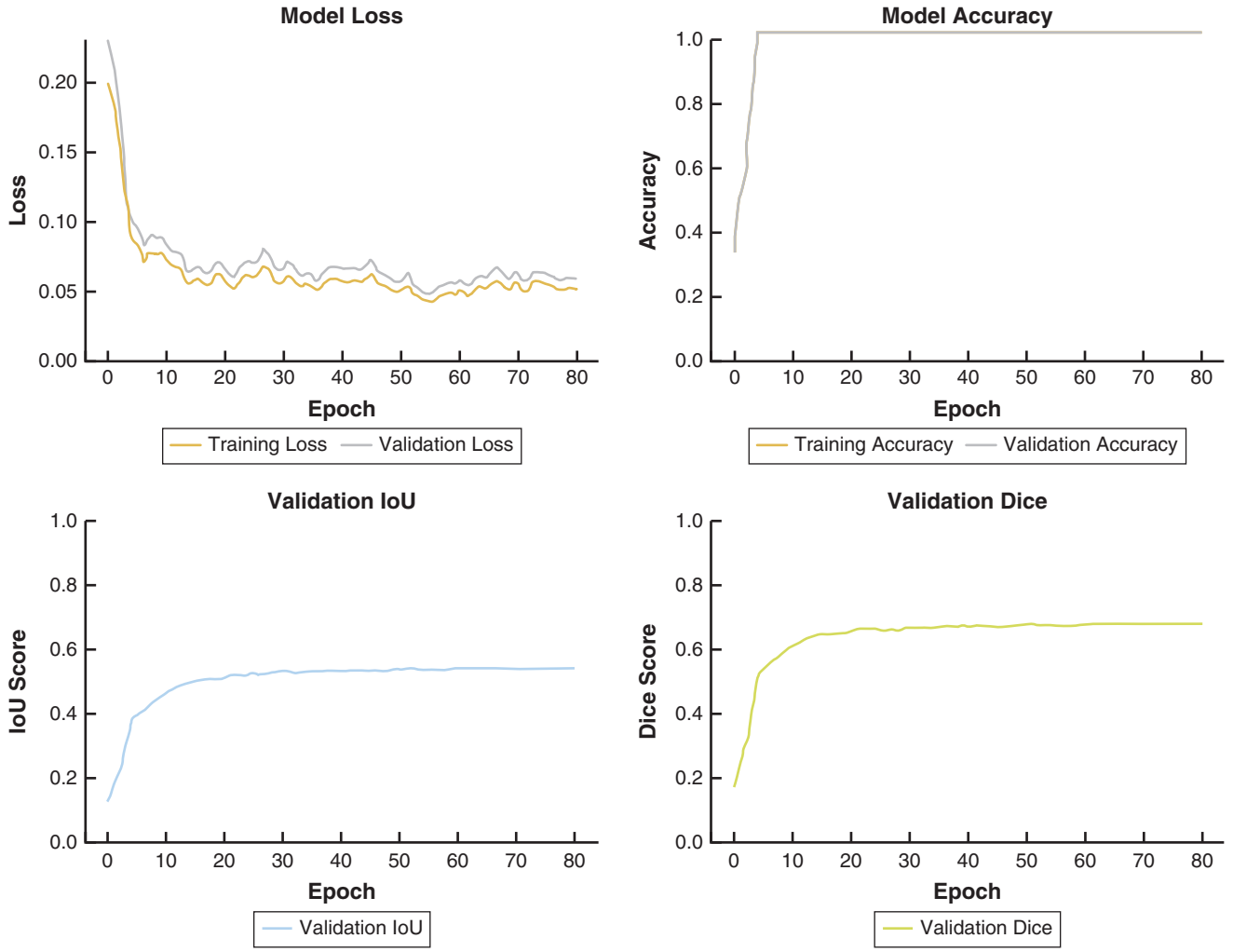


Figure 9. Mask R-CNN dental post training matrix results. Mask R-CNN, region-based convolutional neural network.

(CPU) processing. All models (U-Net segmentation, Mask R-CNN crown-length, and Mask R-CNN post detection) were trained on Kaggle with CUDA-enabled GPUs. Training for more than 100 epochs required approximately 6 hours (U-Net), 8 hours (crown-length Mask R-CNN), and 12 hours (post Mask R-CNN), whereas CPU-only training exceeded 18, 24, and 36 hours, respectively. Per-epoch runtimes were approximately 216, 288, and 432 seconds on GPU versus about 650, 870, and 1300 seconds on CPU. Overall, GPU acceleration reduced development time from several days to less than 1 day and enabled iterative refinement (Table 2).

DISCUSSION

Based on the findings, the research hypothesis that artificial intelligence models can perform radiographic crown lengthening assessment and post selection for the restoration of endodontically treated teeth with accuracy comparable to experienced clinicians was accepted. A modular AI system that automated key radiographic steps in planning restorations for endodontically treated teeth, focusing on 2 decisions: whether crown lengthening is indicated and what post dimensions are appropriate for retention, was introduced. The crown-

Table 1. Deep learning pipeline architecture, dataset size, and performance metrics

Pipeline Component	Architecture	Training Dataset Size	IoU	Dice	Diagnostic Accuracy
Tooth Segmentation	U-Net	598 panoramic images (12,180 instances)	0.52	0.66	—
Crown Measurement Pipeline	Mask R-CNN	1000 representative tooth instances	—	—	0.99 (ferrule presence)
Post Measurement Pipeline	Mask R-CNN	1510 images (70% of 2158 dataset)	0.5237	0.6588	0.9942 (post location identification)

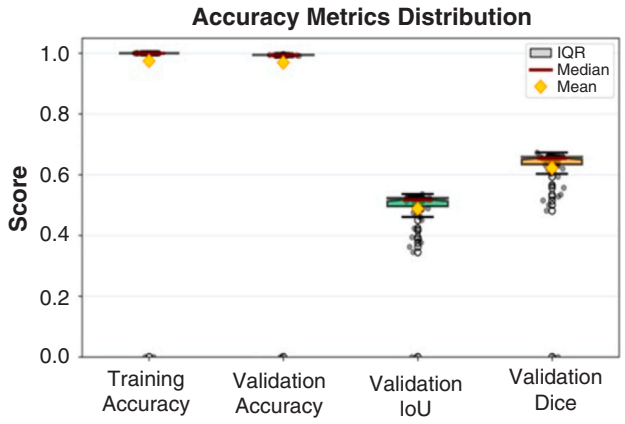


Figure 10. Accuracy and IoU of post model. IoU, intersection over union.

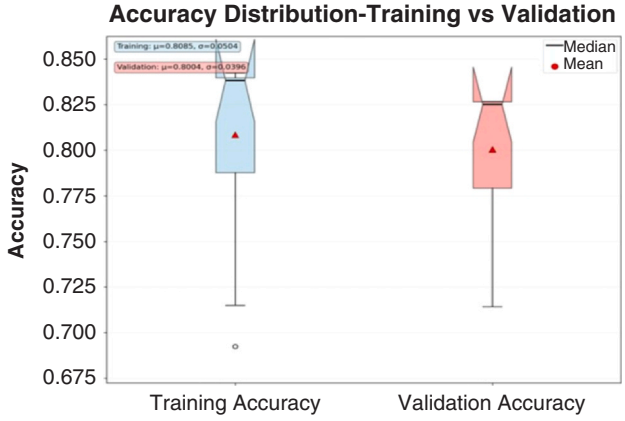


Figure 11. Accuracy of dental crown lengthening model.

length pipeline used Mask R-CNN to measure crown height on pixel-calibrated periapical radiographs, enabling estimation of supracrestal tissue attachment and ferrule. Because inadequate ferrule height (less than 2 mm) has been reported to reduce fracture resistance,[6,7] the model applied these thresholds to output standardized recommendations ("Crown lengthening needed" or "Ready for post and core") consistent with periodontal–restorative protocols.[31–35]

The post-planning pipeline used Mask R-CNN to analyze canal and root morphology and convert bounding-box measurements into clinically interpretable post length and diameter, following established principles (post length approximately two-thirds of root length and diameter no greater than one-third of root width) to support prefabricated or custom post selection, especially in complex anatomy or limited coronal structure.[16–19,21]

Because routine periapical images often lack calibration rulers, pixel-to-millimeter conversion varies with device and projection geometry. Panoramic images add nonuniform magnification, and many public datasets have been distributed as JPEG images without digital imaging and communications in medicine (DICOM) pixel-spacing metadata.[41,42] To address this limitation, the system used marker-free, anatomically referenced calibration through the user interface (tooth type or a reference dimension) to derive an image-specific pixels-per-millimeter factor from expected anatomic dimensions, improving measurement interpretability when markers are absent.[40]

Performance was clinically encouraging (Dice 0.6588; IoU 0.5237; accuracy 0.9942 by epoch 79), aligning with prior convolutional neural network (CNN) based dental imaging work, and U-Net segmentation (Dice and binary cross-entropy loss) supported downstream measurements.[25,30–32]

From a computational perspective, GPU-accelerated training on Kaggle cloud infrastructure reduced model development time. The U-Net model trained in 6 hours on GPU versus over 18 hours on a CPU, and the Mask R-CNN models completed training in 8 and 12 hours versus more than 24 and 36 hours, respectively, on CPU-based environments. Such reductions in training time have been reported in other deep learning studies and are crucial for making AI systems scalable and practical in clinical research environments.[38,39]

The system's modular design, comprising distinct components for segmentation, cropping, detection, and measurement, permitted flexible adaptation. Each component can be independently improved or replaced, allowing integration with other radiographic modalities or 3-dimensional (3D) imaging systems. With further clinical validation, especially in patients with overlapping teeth, edentulous areas, or metallic restorations, this AI pipeline may enhance diagnostic consistency, reduce chair time, and support training of early-career clinicians in prosthodontic and endodontic workflows.

Although the results support feasibility of the proposed workflow for radiographic crown lengthening assessment and post selection, additional external validation across different radiographic systems, acquisition protocols, and clinical settings would further strengthen generalizability. Future work should evaluate performance under challenging radiographic conditions, such as overlap and metallic artifacts, and quantify clinical impact through prospective studies and reader studies assessing time savings and inter-clinician consistency. Incorporating uncertainty estimation for low-confidence cases and integrating a clinician-facing interface may further enhance safe and efficient decision support in restorative planning.

Table 2. Training time comparison (GPU-accelerated versus CPU-only)

Model/Component	GPU Training Time (h)	CPU Training Time (h)
Tooth Segmentation	6	18
Crown Measurement Pipeline	8	24
Post Measurement Pipeline	12	36

CPU, central processing unit; GPU, graphics processing unit.

CONCLUSIONS

Based on the findings of this study, the following conclusions were drawn:

1. A fully automated pipeline was developed to analyze dental radiographs, performing tooth segmentation and isolation, crown-length measurement, and dental-post detection to support restorative dentistry planning.
2. This work contributes to a modular, automated system to improve diagnostic efficiency and may have commercial potential to provide dental professionals and patients with a more efficient approach to post-and-core planning and improved accuracy in dental restorations; however, broader validation on larger, more homogeneous datasets and challenging radiographic scenarios remains necessary.

REFERENCES

1. Reeves WG. Restorative margin placement and periodontal health. *J Prosthet Dent*. 1991;66:733–736.
2. Hempton TJ, Dominici JT. Contemporary crown-lengthening therapy: A review. *J Am Dent Assoc*. 2010;141:647–655.
3. Lanning SK, Waldrop TC, Gunsolley JC, Maynard JG. Surgical crown lengthening: Evaluation of the biological width. *J Periodontol*. 2003;74:468–474.
4. Gargiulo AW, Wentz FM, Orban B. Dimensions and relations of the dentogingival junction in humans. *J Periodontol*. 1961;32:261–267.
5. Schmidt JC, Sahrmann P, Weiger R, Schmidlin PR, Walter C. Biologic width dimensions: A systematic review. *J Clin Periodontol*. 2013;40:493–504.
6. Sorensen JA, Engelman MJ. Ferrule design and fracture resistance of endodontically treated teeth. *J Prosthet Dent*. 1990;63:529–536.
7. Al-Hazaimeh N, Gutteridge DL. An in vitro study into the effect of the ferrule preparation on the fracture resistance of crowned teeth incorporating prefabricated post and composite core restorations. *Int Endod J*. 2001;34:40–46.
8. Fernandes AS, Dessai GS. Factors affecting the fracture resistance of post-core reconstructed teeth: A review. *Int J Prosthodont*. 2001;14:355–363.
9. Khabadze Z, Mordanov O, Taraki F, et al. Effects of the ferrule design on fracture resistance to endodontically treated teeth restored with fiber posts: A systematic review. *Open Dent J*. 2019;13:493–498.
10. Meng Q, Chen Y, Ni K, et al. The effect of different ferrule heights and crown-to-root ratios on fracture resistance of endodontically treated mandibular premolars restored with fiber post or cast metal post system: An in vitro study. *BMC Oral Health*. 2023;23:360.
11. Assiri AYK, Saafi J, Al-Moaleem MM, Mehta V. Ferrule effect and its importance in restorative dentistry: A literature review. *J Popul Ther Clin Pharmacol*. 2022;29:69–82.
12. Majzoub ZAK, Romanos A, Cordioli G. Crown lengthening procedures: A literature review. *Semin Orthod*. 2014;20:188–207.
13. Gupta R, Gupta G, Gupta U, Gupta N. Crown lengthening procedures: A review article. *IOSR J Dent Med Sci*. 2015;14:27–37.
14. Ingber JS. Forced eruption: Alteration of soft tissue cosmetic deformities. *Int J Periodontics Restor Dent*. 1989;9:416–425.
15. Maynard JG, Wilson RDK. Physiologic dimensions of the periodontium significant to the restorative dentist. *J Periodontol*. 1979;50:170–174.
16. Qali M, Alsaegh H, Alsaraf S. Clinical considerations for crown lengthening: A comprehensive review. *Cureus*. 2024;16:e72934.
17. Andrade R, Espinoza M, Gómez EM, Espinoza JR, Cruz E. Intra- and inter-examiner reproducibility of manual probing depth. *Braz Oral Res*. 2012;26:57–63.
18. Fleiss JL, Mann J, Paik M, Goultchin J, Chilton NW. A study of inter- and intra-examiner reliability of pocket depth and attachment level. *J Periodontal Res*. 1991;26:122–128.
19. Choi CH, Back S, Kim S. Effect of X-ray tube angulations and digital sensor alignments on profile angle distortion of CAD-CAM abutments: A pilot radiographic study. *Bioengineering*. 2025;12:772.
20. Li Y, Liu M, Zhou T, Lyu J, Tan J, Liu X. Accuracy of three types of digital guides for crown lengthening surgery: an in vitro study. *J Dent Sci*. 2024;19:39.
21. Rosenstiel SF, Land MF, Walter RD. Contemporary Fixed Prosthodontics. 6th ed.. Elsevier; 2023.
22. Shillingburg HT, Sather DA. Fundamentals of Fixed Prosthodontics. 4th ed.. Quintessence Publishing; 2012.
23. Morgano SM. Restoration of pulpless teeth: Application of traditional principles in present and future contexts. *J Prosthet Dent*. 1996;75:375–380.
24. Lloyd PM, Palik JF. The philosophies of dowel diameter preparation: A literature review. *J Prosthet Dent*. 1993;69:32–36.
25. Gliga A, Imre M, Grandini S, et al. The limitations of periapical X-ray assessment in endodontic diagnosis: A systematic review. *J Clin Med*. 2023;12:4647.
26. Sambrook R, Burrow M. A survey of Australian prosthodontists: The use of posts in endodontically treated teeth. *Aust Dent J*. 2018;63:294–301.
27. Pul U, Schwendicke F. Artificial intelligence for detecting periapical radiolucencies: A systematic review and meta-analysis. *J Dent*. 2024;147:105104.
28. Choi J, Ahn J, Park JM. Deep learning-based automated detection of the dental crown finish line: An accuracy study. *J Prosthet Dent*. 2024;132:1286.e1. –.e9.
29. Kong HJ, Kim YL. Application of artificial intelligence in dental crown prosthesis: A scoping review. *BMC Oral Health*. 2024;24:937.
30. Wimalasiri C., Rathnayake P., Wijerathne S., et al. AI-assisted radiographic analysis in detecting alveolar bone-loss severity and patterns. arXiv 2025:2506.20522.
31. Tuzoff DV, Tuzova LN, Bornstein MM, et al. Tooth detection and numbering in panoramic radiographs using convolutional neural networks. *Dentomaxillofac Radiol*. 2019;48:20180051.
32. Lee JH, Kim DH, Jeong SN, Choi SH. Detection and diagnosis of dental caries using a deep learning-based convolutional neural network algorithm. *J Dent*. 2018;77:106–111.
33. Kuruvilla L, Pawar S, Swargam VT, Mohamed Faizal MR, Sathianath A, Rao V. AI in endodontics: Automated root canal detection and measurement. *J Contemp Clin Pract*. 2025;11:838–842.
34. Rasnayaka S, Leuke Bandara D, Jayasundara A, et al. DenPAR: Annotated intra-oral periapical radiographs dataset for machine learning. *Sci Data*. 2025;12:1615.
35. Rasnayaka S, Bandara DL, Jayasundara A, et al. DenPAR: Annotated intra-oral periapical radiographs dataset. *Zenodo* 2025.
36. Mello Román JC, Fretes VR, Adorno CG, et al. Panoramic dental radiography image enhancement using multiscale mathematical morphology. *Sens (Basel)*. 2021;21:3110.
37. López VRF, Adorno CG, Román JCM, et al. Panoramic radiography database. *Zenodo* 2021.
38. Liu F, Jang H, Kijowski R, Bradshaw T, McMillan AB. Deep learning MR imaging-based attenuation correction for PET/MR imaging. *Radiology*. 2018;286:676–684.
39. Esteva A, Robicquet A, Ramsundar B, et al. A guide to deep learning in healthcare. *Nat Med*. 2019;25:24–29.
40. Shireen A, Ara S. Odontometric analysis of permanent maxillary first molar in gender determination. *J Forensic Dent Sci*. 2016;8:145.
41. Kim YK, Park JY, Kim SG, Kim JS, Kim JD. Magnification rate of digital panoramic radiographs and its effectiveness for pre-operative assessment of dental implants. *Dentomaxillofac Radiol*. 2011;40:76–83.
42. Kahn CE, Langlotz CP, Channin DS, Rubin DL. Informatics in radiology: An information model of the DICOM standard. *Radiographics*. 2011;31:295–304.

Corresponding author:
Dr Lamiaa Said ElFadaly
Faculty of Dentistry
October University for Modern Sciences and Arts
26 July Mehwar Road Intersection with Wahat Road
6th October City
EGYPT
Email: lzaki@msa.edu.eg

CRediT authorship contribution statement
Mohamed Mostafa Rezk: Methodology, Software, Visualization, Validation. **Lamiaa Said Elfadaly**: Supervision, Conceptualization, Project administration, Writing - original draft. **Zeinab Abd Elhalim Taha**: Supervision, Conceptualization, Project administration, Writing - original draft.

Copyright © 2026 by the Editorial Council of *The Journal of Prosthetic Dentistry*. All rights are reserved, including those for text and data mining, AI training, and similar technologies.

https://doi.org/10.1016/j.prosdent.2026.10.009